THE JOURNAL OF PHYSICAL CHEMISTRY B

Article

pubs.acs.org/JPCB

Phenylnaphthalenes: Sublimation Equilibrium, Conjugation, and Aromatic Interactions

Carlos F. R. A. C. Lima,[†] Marisa A. A. Rocha,[†] Bernd Schröder,[‡] Lígia R. Gomes,[§] John N. Low,[∥] and Luís M. N. B. F. Santos*[,†]

[†]Centro de Investigação em Química, Departamento de Química e Bioquímica, Faculdade de Ciências da Universidade do Porto, P-4169-007 Porto, Portugal

[§]CIAGEB-Faculdade de Ciências da Saúde, Escola Superior de Saúde da UFP, Universidade Fernando Pessoa, P-4200-150 Porto, Portugal

[‡]CICECO, Departamento de Química, Universidade de Aveiro, 3810-193 Aveiro, Portugal

[∥]Department of Chemistry, University of Aberdeen, Meston Walk, Old Aberdeen, AB24 3UE, Scotland

Supporting Information

ABSTRACT: In this work, the interplay between structure and energetics in some representative phenylnaphthalenes is discussed from an experimental and theoretical perspective. For the compounds studied, the standard molar enthalpies, entropies and Gibbs energies of sublimation, at T = 298.15 K, were determined by the measurement of the vapor pressures as a function of T, using a Knudsen/quartz crystal effusion apparatus. The standard molar enthalpies of formation in the crystalline state were determined by static bomb combustion calorimetry. From these results, the standard molar enthalpies of formation in the gaseous phase were derived and, altogether with computational chemistry at the B3LYP/6-311++G(d,p) and MP2/cc-pVDZ levels of theory, used to deduce the relative molecular stabilities in various phenylnaphthalenes. X-ray crystallographic structures were obtained for some selected compounds in order to provide structural insights, and relate them to energetics. The thermodynamic quantities for sublimation suggest that molecular symmetry and torsional freedom are major factors affecting entropic differentiation in these molecules, and that cohesive forces are significantly influenced by molecular surface area. The global results obtained support the lack of significant conjugation between aromatic moieties in the α position of naphthalene but indicate the existence of significant electron delocalization when the aromatic groups are in the β position. Evidence for the existence of a quasi T-shaped intramolecular aromatic interaction between the two outer phenyl rings in 1,8-di([1,1′-biphenyl]-4-yl)naphthalene was found, and the enthalpy of this interaction quantified on pure experimental grounds as $-(11.9 \pm 4.8)$ kJ·mol^{-1}, in excellent agreement with the literature CCSD(T) theoretical results for the benzene dimer.

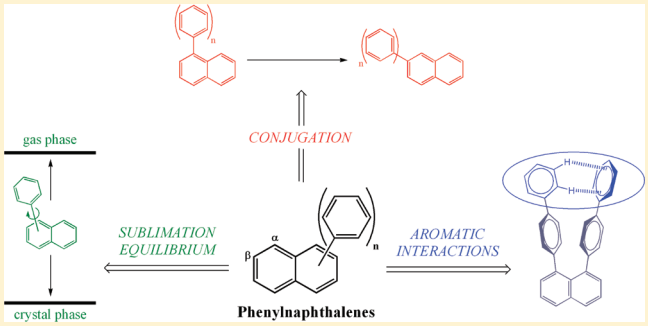

INTRODUCTION

Phenylnaphthalenes are organic compounds consisting of a variable number of phenyl substituents bonded to a unit of naphthalene, as depicted in Figure 1.

Phenylnaphthalenes and related compounds encounter a wide number of applications. They are of interest for the fields of polymer chemistry, nanotechnology, and molecular biology.[1−3] Substituted phenylnaphthalenes can be used as enzyme inhibitors and antibacterial compounds.[4,5]

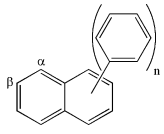

Figure 1. Schematic molecular structure of phenylnaphthalenes, showing the α and β positions of naphthalene.

The relative structural simplicity of phenylnaphthalenes can be explored in order to obtain some fundamental knowledge on the physical−chemical properties of these systems, both in bulk and gas phases. In this work, a systematic study of some phenylnaphthalenes was carried out in order to isolate and characterize the factors that lead to structural and energetic differentiation. These factors are basic physical−chemical phenomena, like enthalpic or entropic effects, electronic delocalization, specific inter and intramolecular interactions, which, although present in many molecular systems, are often superimposed by a myriad of other factors, complicating the task of properly isolating them from the globally intertwined ensemble of phenomena.

Received: November 18, 2011
Revised: January 31, 2012
Published: February 22, 2012

   dx.doi.org/10.1021/jp2111378 | J. Phys. Chem. B 2012, 116, 3557−3570

Figure 2 presents the structures and the abbreviations that will be used throughout this paper for the eight phenyl-

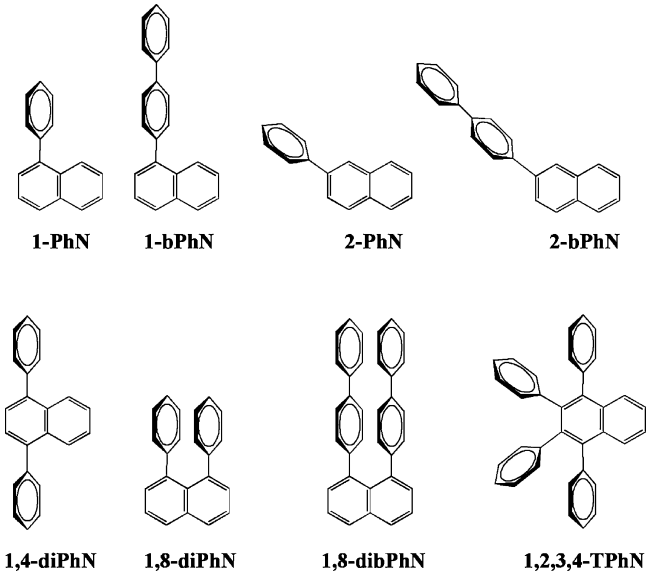

Figure 2. Schematic representation of the phenylnaphthalenes studied in this work and the adopted abbreviations: 1-phenylnaphthalene (1-PhN); 2-phenylnaphthalene (2-PhN); 1-([1,1′-biphenyl]-4-yl)-naphthalene (1-bPhN); 2-([1,1′-biphenyl]-4-yl)naphthalene (2-bPhN); 1,8-diphenylnaphthalene (1,8-diPhN); 1,4-diphenylnaphthalene (1,4-diPhN); 1,8-di([1,1′-biphenyl]-4-yl)naphthalene (1,8-dibPhN); 1,2,3,4-tetraphenylnaphthalene (1,2,3,4-TPhN).

naphthalenes studied. Three groups of structural isomers can be distinguished as follows: A, 1-phenylnaphthalene (1-PhN) and 2-phenylnaphthalene (2-PhN); B, 1-([1,1′-biphenyl]-4-yl)-naphthalene (1-bPhN), 2-([1,1′-biphenyl]-4-yl)naphthalene (2-bPhN), 1,8-diphenylnaphthalene (1,8-diPhN) and 1,4-diphenylnaphthalene (1,4-diPhN); C, 1,8-di([1,1′-biphenyl]-4-yl)naphthalene (1,8-dibPhN) and 1,2,3,4-tetraphenylnaphthalene (1,2,3,4-TPhN). This subdivision is useful because more direct comparisons can be made between isomers, and chemical stability can only be meaningfully compared within the same potential energy surface (PES).

The presence of aromatic moieties can induce an extensive conjugation along the π systems, which is associated with charge delocalization and electronic correlation, and may lead to significant molecular stabilization. Additionally, the existence of adjacent phenyl substituents (like in 1,8-diPhN), opens the possibility for considerable intramolecular steric repulsions and/or aromatic interactions. Aromatic interactions are non-covalent intra- and/or intermolecular interactions involving at least one aromatic system. The relatively large polarizability of aromatics and the quadrupole moment created by the interplay between the σ and π frameworks of an aromatic group can lead to the establishment of significant dispersive van der Waals and electrostatic interactions, respectively.[6−11] Three types of structures are generally observed for the interaction between two aromatic groups: T-shaped (T), parallel-displaced (PD), and stacked (S).[8,9,11] The T structure is in its essence a C−H···π interaction.[8,11,12] Aromatic interactions are cohesive forces present in the bulk phases of aromatic compounds, and they have an irrefutable importance in molecular recognition processes and in defining the conformation of molecules and macromolecules, like proteins or DNA.[9,13,14] Aromatic interactions are also a hot topic in supramolecular chemistry.[9,15,16]

This work is a combined structural/energetic study of this family of compounds, comprising the following: X-ray crystallography for the determination of crystal phase structures; Knudsen/quartz crystal effusion for vapor pressure measurement as a function of T, and consequent derivation of the thermodynamic quantities of sublimation; combustion calorimetry for evaluation of the enthalpies of formation of the crystalline compounds, and consequent derivation of the enthalpies of formation in the gas phase in combination with the sublimation data; UV−vis spectroscopy for exploring the electronic properties of some relevant phenylnaphthalenes; a computational study, using B3LYP and MP2 methods, as a support of the experimental results and assessment of gas phase geometries and energetics.

A series of homodesmotic reaction schemes is used in order to detect and quantify, on pure experimental grounds, some important electronic effects that can influence energetics in some of the molecules under study.

EXPERIMENTAL SECTION

Synthesis, Purification, and Characterization of the Studied Compounds. 1,2,3,4-Tetraphenylnaphthalene was commercially obtained from Sigma-Aldrich, washed with boiling methanol and sublimed under reduced pressure. All the other compounds, excluding 1,4-diphenylnaphthalene, were synthesized and purified as described elsewhere.[17,18]

1,4-Diphenylnaphthalene. A 40 mL solution of K_2CO_3 (28 mmol) in water was added to a solution of 1,4-dibromonaphthalene (7 mmol), phenylboronic acid (25 mmol) and palladium acetate (2 mol %) in 40 mL of DMF. The resultant solution was stirred at 90 °C for 9 h. The crude product was extracted with ethyl acetate. The organic phase was washed with water and NaOH(aq) 1 M, and evaporated yielding a yellowish solid (yield (%) = 66). The compound was washed with boiling methanol and sublimed under reduced pressure to yield pure white crystals of 1,4-diPhN (mp = 134.8−135.7 °C). ^{1}H NMR (400 MHz, $CDCl_3$, 300 K, TMS): 8.01 (2H, dd, H_5 and H_8, J_{ortho} = 6.5, J_{meta} = 3.3), 7.61−7.44 (14 H, m); ^{13}C NMR (100.6 MHz, $CDCl_3$, 300 K): 141.7, 140.8, 132.8, 131.1, 129.2, 128.2, 127.4, 127.3, 126.8.

The purity of the compounds was verified by gas−liquid chromatography, using an HP 4890 apparatus equipped with a HP-5 column, cross-linked, 5% diphenyl and 95% dimethylpolysiloxane, showing a %(m/m) purity greater than 99.8% for all the compounds.

Structural Characterization. Crystals suitable for X-ray diffraction of 1-bPhN were grown from evaporation of a CH_2Cl_2/isooctane (1:1) solution. Crystals of 1,8-dibPhN and 1,8-diPhN were grown from evaporation of a CH_2Cl_2 solution. Crystals of 1,4-diPhN were grown from evaporation of a CH_2Cl_2/acetone (1:1) solution. The intensity data was collected in a Bruker-Nonius CCD diffractometer. Data collection, cell refinement and data reduction were made with the software package of the diffractometer: *APEX2 and SAINT*.[19] Absorption correction was performed with *SADABS*.[19] The structure was solved and refined using the following software: *OSCAIL*[20] and *SHELXL97*.[21] H atoms were treated as riding atoms with C−H(aromatic), 0.95 Å. The crystal of 1,4-diphenylnaphthalene was a merohedral twin with a twin component ratio of 66/34. Molecular graphics were made with *ORTEP*[22] and *PLATON*.[23] The complete set of

dx.doi.org/10.1021/jp2111378 | J. Phys. Chem. B 2012, 116, 3557−3570

structural parameters in CIF format is available as an Electronic Supplementary Publication from the Cambridge Crystallographic Data Centre, CCDC: 698100 (1-bPhN), 668280 (1,8-dibPhN), and 802922 (1,4-diPhN). Information about crystal data, data acquisition conditions and refinement parameters for these compounds is given as Supporting Information. Despite all efforts, crystals suitable for X-ray diffraction for 2-PhN and 2-bPhN could not be obtained.

UV−Vis Spectroscopy. UV−vis spectra for 1-PhN (1.835×10^{-5} mol·dm^{-3}), 2-PhN (1.995×10^{-5} mol·dm^{-3}), 1-bPhN (1.576×10^{-5} mol·dm^{-3}), and 2-bPhN (1.379×10^{-5} mol·dm^{-3}), in the region of (190−1090) nm, in CH_2Cl_2 were measured with an Agilent 8453 diode array UV−vis spectrometer, at T = 298.1 K; the molar concentrations are given in parentheses. A quartz cell with a path length of 10.00 mm was used. Temperature control was achieved by means of a Julabo F25 HP refrigerated circulator.

Combustion Calorimetry. *1-([1,1′-Biphenyl]-4-yl)-naphthalene.* The standard molar enthalpy of combustion, $\Delta_c H^o_m$, at T = 298.15 K, was measured in an isoperibol static bomb combustion calorimeter with a twin valve bomb of internal volume of 0.290 dm^3, formerly used at the National Physical Laboratory, Teddington, U.K. The measurements were performed mainly as previously described, although a few changes in technique, due to different auxiliary equipment, were applied.[24,25]

Other Compounds. The standard molar enthalpies of combustion, $\Delta_c H^0_m$, at T = 298.15 K, were measured in an isoperibol mini-bomb combustion calorimeter.[26] The mini-bomb is made of stainless steel with 0.46 cm wall thickness and 18.2 cm^3 of internal volume. The internal fittings located on the head of the mini-bomb (electrodes, crucible support and sheet) are all made of platinum.

The program LABTERMO[27] was used to compute the corrected adiabatic temperature change, ΔT_{ad}. The densities, in g·cm^{-3}, of the compounds were taken from the crystallographic data presented in this work and in the literature: 1-bPhN, 1.25; 1,4-diPhN, 1.26; 1,8-diPhN, 1.14;[28] 1,8-dibPhN, 1.28; 1,2,3,4-TPhN, 1.19;[29] 2-PhN, 1.25 (considered the same as for 1-bPhN); 2-bPhN, 1.25 (considered the same as for 1-bPhN). The values of $(\partial u/\partial p)_T$ at T = 298.15 K were assumed to be 0.2 J·g^{-1}·MPa^{-1}.[30,31] The corresponding energetic correction usually leads to negligible errors in the final combustion results. Standard state corrections were calculated for the initial and final states by the procedures given by Hubbard et al.[32] and by Good and Scott.[33] The relative atomic masses used were those recommended by the IUPAC Commission in 2005.[34]

Knudsen/Quartz Crystal Effusion. The vapor pressures of the studied compounds were measured as a function of temperature by the combined Knudsen/quartz crystal effusion method recently developed in our laboratory.[35] This technique is based on the simultaneous gravimetric and quartz crystal microbalance mass loss detection, enabling the use of a temperature-step methodology, and having the advantages of smaller sample sizes and effusion times, and the possibility of achieving temperatures up to 650 K. In a typical Knudsen effusion experiment, the system is kept at high vacuum, enabling free effusion of the vapor from the cell, while the oven is kept at a fixed temperature, T.

Computational Details. All theoretical calculations were performed using the Gaussian 03 software package.[36] The full geometry optimizations were performed using the Moller−Plesset perturbation theory with a second order perturbation (MP2) and the correlation consistent basis set cc-pVDZ, and density functional theory (DFT) with the hybrid exchange correlation functional (B3LYP) and the 6-311++G(d,p) basis set. The spin-component-scaled MP2 approach (SCS-MP2)[37] was also used for the calculation of the ground-state electronic energies. Some of the phenylnaphthalenes studied are prone to establish intramolecular dispersive interactions. For that reason were chosen a method that is virtually blind to these interactions (B3LYP) and one that can describe them satisfactorily (MP2), for then the presence of such interactions in one molecule will probably lead to a significant discrepancy between the B3LYP and MP2 results.

RESULTS

X-ray Crystallographic Structures. The X-ray structure determination for 1-bPhN, 1,8-dibPhN, 1,4-diPhN, and 1,8-diPhN confirmed the expected molecular structures. A literature search revealed that the crystalline structures for 1,8-diPhN[28] and 1,2,3,4-TPhN[29] have been previously determined. The geometrical parameters and supramolecular structure obtained in this work, corresponding to low temperature data acquisition of 1,8-diPhN, compares well with the structural data published by Tsuji et al. at room temperature and thus it will not be discussed here.[28] The molecular structures for 1,4-diPhN, 1,8-dibPhN, and 1-bPhN are presented in Figures 3−5.

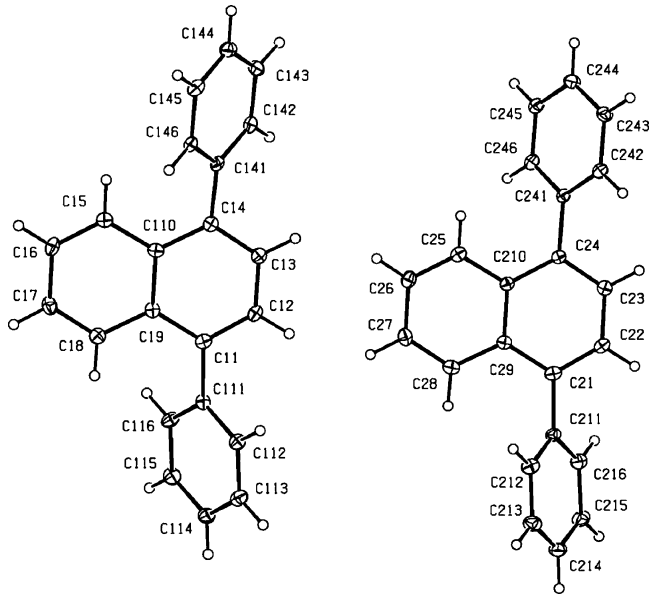

Figure 3. View of 1,4-diPhN with our numbering scheme. Displacement ellipsoids are drawn at the 30% probability level. Molecule 1 with C1X labels and molecule 2 with C2X labels.

Compound 1,4-diPhN crystallizes with two molecules on the asymmetric unit whose carbon atoms are labeled as C1X and C2X for molecule 1 and molecule 2, respectively. The main bond lengths for the compounds are within the expected range for aromatics. The distances found for C−C bonds of the phenyl rings show values within the typical range of 1.384(13) Å, corresponding to the mean value for the C_{ar}−C_{ar} bond in aromatic compounds.[38] Nevertheless, a significant elongation of the C9−C10 bond length on the naphthalene ring in 1,8-dibPhN (1.439(3) Å) and 1,4-diPhN (1.442(7) and 1.436(7) Å) is observed when compared with the corresponding value

dx.doi.org/10.1021/jp2111378 | J. Phys. Chem. B 2012, 116, 3557−3570

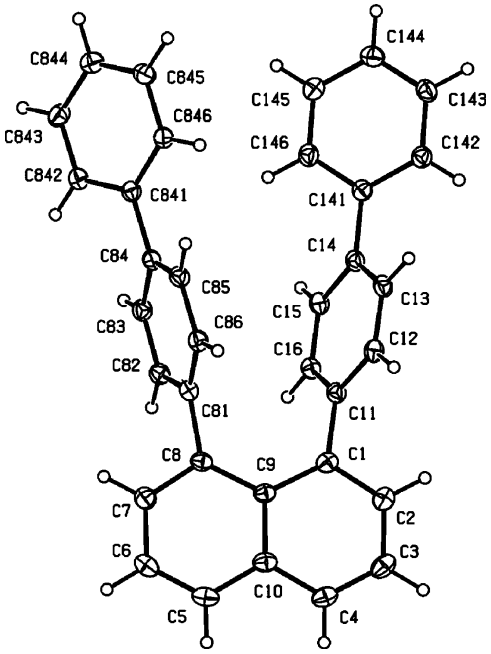

Figure 4. View of 1,8-dibPhN with our numbering scheme. Displacement ellipsoids are drawn at the 30% probability level.

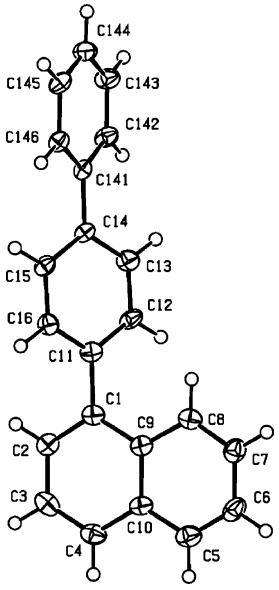

Figure 5. View of 1-bPhN with our numbering scheme. Displacement ellipsoids are drawn at the 30% probability level.

for naphthalene at 135 K (1.424(2)) Å.[39] For compound 1-bPhN, no significant differences in the geometrical parameters of the naphthalene ring is observed when compared with naphthalene in spite of the 1,1′-biphenyl substitution. Table 1 shows the dihedral angles between the mean planes of the phenyl rings and the naphthalene ring for the characterized compounds, and for 1,8-diPhN[28] and 1,2,3,4-TPhN.[29] Compounds with phenyl rings inserted in *ortho* or *peri* positions of the naphthalene moiety show higher dihedral angles. This variation lies within the 11° to 23° range reflecting the expected higher steric hindrance of *ortho*/*peri* substitution.

Table 2 shows the dihedral angles between the mean planes of each of the phenyl rings for 1-bPhN and 1,8-dibPhN.

The supramolecular structures of 1-bPhN and 1,8-dibPhN are stabilized by three C−H···π intermolecular interactions, whereas in 1,4-diPhN there are no significant C−H···π or π···π interactions. The geometric parameters for the interactions are summarized in Table 3 and depicted in Figures 6−8.

In 1-bPhN the center of gravity of the C1−C2−C3−C4−C9−C10 aromatic ring of the naphthalene moiety acts as acceptor for two short C−H···π interactions from which the donor H atoms are the *ortho* hydrogens attached to the outer biphenyl ring. These link symmetry related molecules into chains running parallel to the *a*-axis (Figure 6). A third and longer C(7)−H(7)···π(141) interaction involving the C7−H7 donor of the naphthalene ring and the center of gravity of the C141−C146 phenyl ring links the previous chains to form sheets lying parallel to the *ab* plane (Figure 6). Similarly, in 1,8-dibPhN, it is the C1−C2−C3−C4−C9−C10 aromatic ring of the naphthalene moiety located at (x, y, z) that is the acceptor of two C−H···π interactions: one involving the C4−H4 donor of the naphthalene ring at ($0.5 - x$, $-0.5 + y$, $0.5 - z$), linking the molecules in antiparallel chains, and one involving the C15−H15 acceptor located at (x, $1 + y$, z) that links the two molecules into a chain along the *b*-axis by a unit translation (Figure 7). These chains are then linked by a third C(844)−H(844)···π(141) interaction to form a sheet which lies parallel to the *bc* plane (Figure 8). It is interesting to note that the D−A···A angular values (Table 3) for the shorter C−H···π interactions in 1,8-dibPhN show that they are practically coaxial, favoring the electrostatic dipole−quadrupole contribution for this type of interaction.[8−11]

Combustion Calorimetry. The detailed results for combustion calorimetry of the compounds studied are provided as Supporting Information. The products of combustion in the experiments consist of a gaseous phase and an aqueous mixture for which the thermodynamic properties are known. The values of $\Delta_c U^0_m$ refer to the combustion reactions of the studied compounds, represented by the general equation:

$$C_nH_m(cr) + (n + m/4)O_2(g) \rightarrow nCO_2(g) + (m/2)H_2O(l) \quad (1)$$

Table 4 lists the derived standard molar energies of combustion, $\Delta_c U^0_m(cr)$, the standard molar enthalpies of combustion, $\Delta_c H^0_m(cr)$, and the standard molar enthalpies of formation, $\Delta_f H^0_m(cr)$, of the crystalline solids. In accordance with normal thermochemical practice, the uncertainties assigned to $\Delta_c H^0_m(cr)$ and $\Delta_f H^0_m(cr)$ are twice the overall standard deviation of the mean and include the uncertainties in calibration and in the auxiliary quantities used. To derive $\Delta_f H^0_m(cr)$ from $\Delta_c H^0_m(cr)$, the standard molar enthalpies of formation of $H_2O(l)$ and $CO_2(g)$ at T = 298.15 K, $-(285.830 \pm 0.042)$ kJ mol^{-1} and $-(393.51 \pm 0.13)$ kJ mol^{-1}, respectively, were used.[40]

Heat Capacity Measurements and Estimations. The values of $C^o_{p,m}(cr)$, at T = 298.15 K, were measured for 1,4-diPhN and 1,2,3,4-TPhN using a high-precision heat capacity drop calorimeter, developed by Wadsö[41,42] at the Thermochemistry Laboratory of Lund, Sweden, afterward transferred to Porto, Portugal, in where it was modernized with regards to the temperature sensors and electronics, and enabling the use of computer data acquisition in a user-friendly environment.[43] For

dx.doi.org/10.1021/jp2111378 | J. Phys. Chem. B 2012, 116, 3557−3570

Table 1. Dihedral Angles between the Mean Planes of the Phenyl Rings and the Naphthalene Ring for the Characterized Compounds and for 1,8-diPhN[28] and 1,2,3,4-TPhN[29]

	dihedral angles/deg				
	C1[a]	C2[a]	C3[a]	C4[a]	C8[a]
1-bPhN	56.52(11)	–	–	–	–
1,8-dibPhN	60.64(9)	–	–	–	73.80(9)
1,4-diPhN	53.1(2)	–	–	50.4(2)	–
	52.2(2)	–	–	54.2(2)	–
1,8-diPhN	66.48(10)	–	–	–	67.10(10)
1,2,3,4-TPhN	66.50(7)	68.81(8)	65.17(8)	71.48(8)	–
	76.04(8)	62.55(8)	62.55(8)[b]	76.04(8)[b]	–

[a]Attachment atom position. [b]There are 1.5 molecules in the asymmetric unit. One of the molecules sits on a 2-fold crystallographic axis, which bisects the naphthalene moiety lengthwise.

Table 2. Dihedral Angles between the Mean Planes of Each of the Phenyl Rings for 1-bPhN and 1,8-dibPhN

	dihedral angles/deg	
	C14[a]	C84[a]
1-bPhN	28.23(12)	
1,8-dibPhN	42.34(9)	30.05(11)

[a]Attachment atom position.

Table 3. Intermolecular Interactions, Distances, and Angles (Å and deg)[a]

compound	D−H···A	H···A /Å	D···A/Å	D−A···A /°
1-bPhN	C(7)−H(7)···π(141)^{i}	2.94	3.708(3)	139
	C(142)−H(142)···π(1)^{ii}	2.79	3.599(3)	143
	C(146)−H(146)···π(1)^{iii}	2.71	3.565(3)	150
1,8-dibPhN	C(4)−H(4)···π(1)^{iv}	2.75	3.691(3)	172
	C(15)−H(15)···π(1)^{v}	2.87	3.679(3)	144
	C(844)−H(844)···π(141)^{vi}	2.64	3.587(3)	174

[a]π(141) is the centroid of the C141−C146 ring, π(1) is the centroid of the C1−C2−C3−C4−C9−C10 ring of naphthalene. Symmetry codes: (*i*) $x, -1 + y, z$; (*ii*) $-x, {}^{1}/_{2} + y, {}^{1}/_{2} - z$; (*iii*) $1 - x, {}^{1}/_{2} + y, {}^{1}/_{2} - z$; (*iv*) ${}^{1}/_{2} - x, {}^{1}/_{2} + y, {}^{1}/_{2} - z$; (*v*) $x, -1 + y, z$; (*vi*) $-{}^{1}/_{2} - x, -{}^{1}/_{2} + y, {}^{3}/_{2} - z$.

the other compounds, $C^{o}_{p,m}$(cr), at T = 298.15 K, was estimated by an additive method based on the equation:

$$C^{o}_{p,m}(\text{compound, cr}) = C^{o}_{p,m}(\text{naphthalene, cr}) + n(\text{Ph})C^{o}_{p,m}(\text{Ph increment, cr}) \quad (2)$$

where $C^{o}_{p,m}$(naphthalene, cr) = 165.7 J·K^{-1}·mol^{-1}, n(Ph) is the number of phenyl substituents in the compound, and $C^{o}_{p,m}$(Ph increment, cr) is the mean value for the increment in $C^{o}_{p,m}$(cr) per phenyl ring, estimated by a least-squares method, using the experimental values of $C^{o}_{p,m}$(cr) for: naphthalene (165.7), 1,4-diPhN, 1,2,3,4-TPhN, biphenyl (198.4), *o*-terphenyl (274.8), *p*-terphenyl (278.7), *p*-quaterphenyl (362.5), and 1,3,5-triphenylbenzene (361.0); all values in parentheses are in J·K^{-1}·mol^{-1} and were taken from Domalski.[44] The theoretical values of $C^{o}_{p,m}$(g), at T = 298.15 K, for 1-bPhN, 1,4-diPhN, and 1,8-diPhN were computed at the B3LYP/6-311++G(d,p) level of theory using the scaling factor of 0.9688 for the fundamental frequencies calculations.[45] Correction for hindered rotation of the phenyl groups was not considered since it is generally of relatively small magnitude and lies within the uncertainties derived for the $\Delta^{g}_{cr}C^{o}_{p,m}$ values. For the other compounds $C^{o}_{p,m}$(g) was calculated according to an equation analogous to

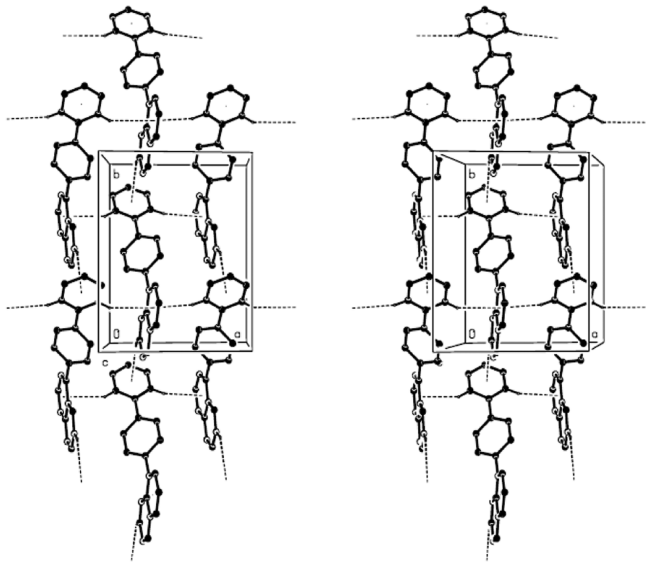

Figure 6. View of the supramolecular structure of 1-bPhN, showing the C−H···π intermolecular interactions. Hydrogen atoms not involved in the motifs are not included.

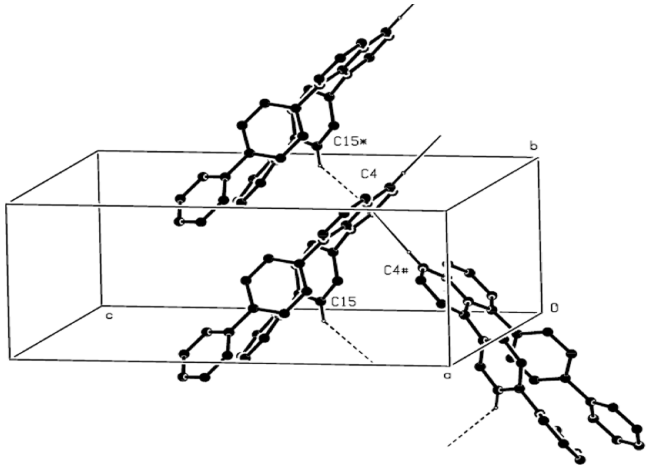

Figure 7. View of the supramolecular structure of 1,8-dibPhN, showing the C−H···π intermolecular interactions. Hydrogen atoms not involved in the motifs are not included.

dx.doi.org/10.1021/jp2111378 | J. Phys. Chem. B 2012, 116, 3557−3570

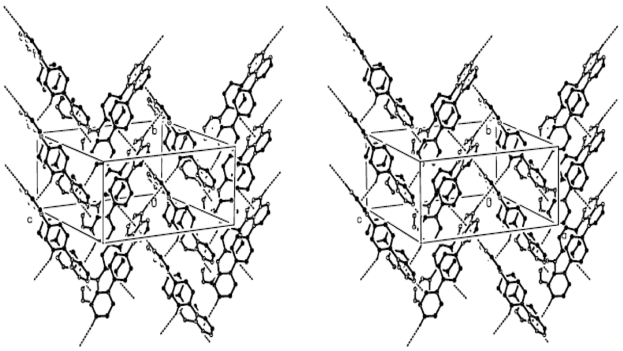

Figure 8. View of the supramolecular structure of 1,8-dibPhN, showing the sheets that lie parallel to the *bc* plane. Hydrogen atoms not involved in the motifs are not included.

Table 4. Derived standard (p^0 = 10^5 Pa) Molar Energies of Combustion, $\Delta_c U^0_m$(cr), Standard Molar Enthalpies of Combustion, $\Delta_c H^0_m$(cr), and Standard Molar Enthalpies of Formation, $\Delta_f H^0_m$(cr), in the Crystalline State, at T = 298.15 K, for the Compounds Studied

	$\Delta_c U^0_m$(cr)/kJ mol^{-1}	$\Delta_c H^0_m$(cr)/kJ mol^{-1}	$\Delta_f H^0_m$(cr)/kJ mol^{-1}
2-PhN	−8143.9 ± 2.2	−8151.3 ± 2.2	140.2 ± 3.0
1-bPhN	−11145.9 ± 3.0	−11155.8 ± 3.0	212.0 ± 4.2
2-bPhN	−11132.2 ± 2.9	−11142.2 ± 2.9	198.3 ± 4.1
1,4-diPhN	−11156.7 ± 3.2	−11166.6 ± 3.2	222.7 ± 4.3
1,8-diPhN	−11177.4 ± 3.2	−11187.4 ± 3.2	243.5 ± 4.3
1,8-dibPhN	−17171.1 ± 4.8	−17186.0 ± 4.8	376.7 ± 6.5
1,2,3,4-TPhN	−17204.1 ± 4.6	−17219.0 ± 4.6	409.7 ± 6.4

eq 2, using the following calculated values of $C^o_{p,m}$(g) (at the same level of theory) for the estimation of $C^o_{p,m}$(Ph increment, g) by a least-squares method: naphthalene (134.2), 1-PhN (217.6), 2-PhN (217.8), 1-bPhN (300.8), 2-bPhN (301.2), 1,4-diPhN (300.5), and 1,8-diPhN (300.9); all values are in J·K^{-1}·mol^{-1}. For the least-squares methods the average errors of 1.9 (for $C^o_{p,m}$(cr)) and of 0.1 (for $C^o_{p,m}$(g)) between the experimental/theoretical and estimated heat capacities were obtained, corresponding respectively to approximately 0.6% and 0.05% deviation. The uncertainties in the estimated and theoretically calculated heat capacities were assumed to be of ±2.0 J·K^{-1}·mol^{-1} for $C^o_{p,m}$(cr) and of ±5.0 J·K^{-1}·mol^{-1} for $C^o_{p,m}$(g). The global heat capacities results of the compounds studied are presented in Table 5.

Knudsen/Quartz Crystal Effusion. For some of the compounds studied, the standard molar enthalpies, $\Delta^g_{cr}H^0_m$, and entropies, $\Delta^g_{cr}S^0_m$, of sublimation at the mean temperature, ⟨T⟩, were derived using the integrated form of the Clausius−Clapeyron equation:

$$\ln p = a - b/T \tag{3}$$

where a is a constant and $b = \Delta^g_{cr}H_m(\langle T\rangle)/R$. Figure 9 presents the plots of ln (p/Pa) = f (T^{-1}/K^{-1}) for the compounds studied, obtained in the Knudsen/quartz crystal effusion apparatus, recently developed in our laboratory.[35]

The detailed experimental results are given as Supporting Information. The molar enthalpy of sublimation, $\Delta^g_{cr}H_m$, at the mean temperature, ⟨T⟩, was derived from the parameter b of the Clausius−Clapeyron equation, and the molar entropy of sublimation at $p(\langle T\rangle)$ and at ⟨T⟩, $\Delta^g_{cr}S_m(\langle T\rangle, p(\langle T\rangle))$, is calculated as:

$$\Delta^g_{cr}S_m(\langle T\rangle, p(\langle T\rangle)) = \Delta^g_{cr}H_m(\langle T\rangle)/\langle T\rangle \tag{4}$$

The standard molar enthalpy of sublimation, $\Delta^g_{cr}H^0_m$, at T = 298.15 K is determined by eq 5:

$$\Delta^g_{cr}H^o_m(298.15\ \text{K}) = \Delta^g_{cr}H_m(\langle T\rangle) + (298.15 - \langle T\rangle)\Delta^g_{cr}C^o_{p,m} \tag{5}$$

where:

$$\Delta^g_{cr}C^o_{p,m} = C^o_{p,m}(g) - C^o_{p,m}(cr) \tag{6}$$

The values for the heat capacities, $C^o_{p,m}$(cr) and $C^o_{p,m}$(g), are those presented in Table 5. The standard molar entropy of sublimation, $\Delta^g_{cr}S^0_m$, at T = 298.15 K, was calculated according to eq 7:

$$\Delta^g_{cr}S^0_m(298.15\ \text{K}) = \Delta^g_{cr}S_m(\langle T\rangle, p(\langle T\rangle)) + \Delta^g_{cr}C^0_{p,m} \ln(298.15/\langle T\rangle) - R\ln\{p^0/p(\langle T\rangle)\} \tag{7}$$

where p^o = 10^5 Pa.

Table 5. Heat Capacities, $C^o_{p,m}$(cr) and $C^o_{p,m}$(g), at T = 298.15 K, for the Compounds Studied

	$C^o_{p,m}$(cr)/J·K^{-1}·mol^{-1}	$C^o_{p,m}$(g)/J·K^{-1}·mol^{-1}
1-bPhN	328.3 ± 2.0[a]	300.8 ± 5.0
1,4-diPhN	324.0 ± 1.4	300.5 ± 5.0
1,8-diPhN	328.3 ± 2.0[a]	300.9 ± 5.0
1,8-dibPhN	490.9 ± 2.0[a]	467.9 ± 5.0[a]
1,2,3,4-TPhN	491.6 ± 0.9	467.9 ± 5.0[a]

[a]Estimated values (see text).

DISCUSSION

Data Compilation. A compilation of all relevant thermodynamic data, at T = 298.15 K, for the phenylnaphthalenes studied in this work and naphthalene is given in Table 6. The standard molar enthalpies of formation in the gas phase, $\Delta_f H^0_m$(g), at T = 298.15 K, for the compounds studied, were calculated according to eq 8:

$$\Delta_f H^0_m(g, 298.15\ \text{K}) = \Delta_f H^0_m(cr, 298.15\ \text{K}) + \Delta^g_{cr}H^0_m(298.15\ \text{K}) \tag{8}$$

Sublimation Thermodynamics. The data presented in Table 6 clearly indicates the existence of a significant differentiation in the enthalpies and entropies of sublimation among the studied phenylnaphthalenes.

In these compounds the entropy of sublimation can be approximately dissected into the following terms:

1. The increase in $\Delta^g_{cr}S^0_m$ due to the presence of additional phenyl substituents.
2. Molecular symmetry: higher symmetry leads to higher S^0(cr) (more symmetry increases the number of atomic permutations by molecular rotation that are compatible with a given macrostate, thus increasing the number of ways into which the crystal lattice can be realized—this is valid since a unique set of coordinates within the lattice can be attributed to each atom, and thus each atom in the

dx.doi.org/10.1021/jp2111378 | J. Phys. Chem. B 2012, 116, 3557−3570

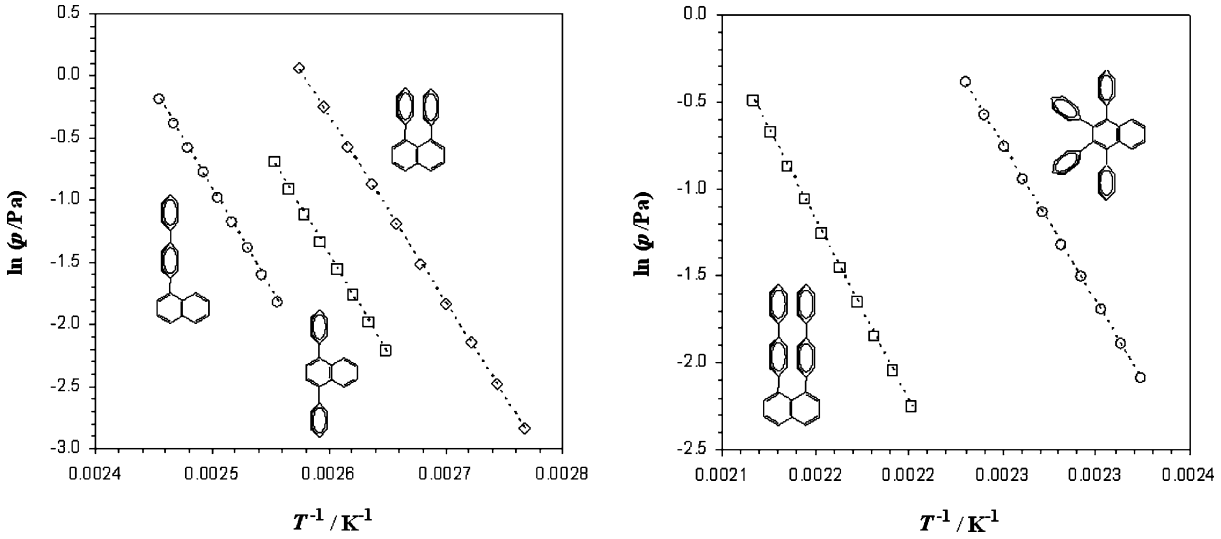

Figure 9. Plots of $\ln(p/\mathrm{Pa}) = f\,(T^{-1}/\mathrm{K}^{-1})$ for the compounds studied, obtained in the Knudsen/quartz crystal effusion apparatus.

Table 6. Compilation of Relevant Thermodynamic Data, at T = 298.15 K, for the Phenylnaphthalenes Studied in This Work and Naphthalene

compound	$\Delta_{cr}^{g}H_m^0$/kJ mol^{-1}	$\Delta_{cr}^{g}S_m^0$/J·K^{-1}·mol^{-1}	$\Delta_f H_m^0$(g)/kJ mol^{-1}
naphthalene	72.70 ± 0.04[46]	168.1 ± 0.1[46]	150.6 ± 1.5[47]
1-PhN	–	–	252.3 ± 3.4[a]
2-PhN	107.8 ± 0.6[17]	211.5 ± 1.8[17]	248.0 ± 3.1
1-bPhN	138.9 ± 0.8	245.0 ± 2.1	350.9 ± 4.3
2-bPhN	140.2 ± 1.3[17]	228.0 ± 3.6[17]	338.5 ± 4.3
1,4-diPhN	132.5 ± 0.6	237.4 ± 1.6	355.2 ± 4.3
1,8-diPhN	126.4 ± 0.5	230.9 ± 1.4	369.9 ± 4.3
1,8-dibPhN	178.5 ± 1.1	280.2 ± 2.7	555.2 ± 6.6
1,2,3,4-TPhN	154.2 ± 0.8	246.9 ± 2.1	563.9 ± 6.4

[a]Estimated value (see details in the text).

crystal is distinguishable from all the others), and/or lower S^0(g) (the Pauli exclusion principle does not allow microscopically indistinguishable rotational states in a symmetric molecule), therefore decreasing $\Delta_{cr}^{g}S_m^0$.[48−60]

3. The internal rotational freedom of the phenyl substituents in the gas phase: higher barrier heights being associated with a decrease of S^0(g), and thus a decrease in $\Delta_{cr}^{g}S_m^0$.

The molecules of 1-bPhN and 2-bPhN belong to the C_1 symmetry point group, having associated a symmetry number of 1, σ_{sym} = 1. On the contrary, the X-ray structures of 1,8-diPhN and 1,4-diPhN present a molecular geometry consistent with the C_2 point group, for which σ_{sym} = 2. This nonthermal entropic contribution should decrease $\Delta_{cr}^{g}S_m^0$ by about R ln(2) = 5.8 J·K^{-1}·mol^{-1}, either by increasing S^0(cr), decreasing S^0(g), or a combination of both to varying extents.[60−64] Because of the presence of one adjacent phenyl neighbor, the barrier height associated with hindered phenyl rotation in 1,8-diPhN should be significantly higher than in the other isomers and contribute to a decrease in S^0(g), and hence in $\Delta_{cr}^{g}S_m^0$. For the decrease in S^0(g) to be directly reflected in $\Delta_{cr}^{g}S_m^0$, one must assume that in the solid phase the respective vibrational modes are hindered to the same extent in all isomers, having very high rotational barriers due to the constraints imposed by the crystal lattice. It can also be assumed that the phenyl internal rotations in gaseous 1-bPhN and 1,4-diPhN are rather alike. Figure 10 illustrates the reasoning presented above.

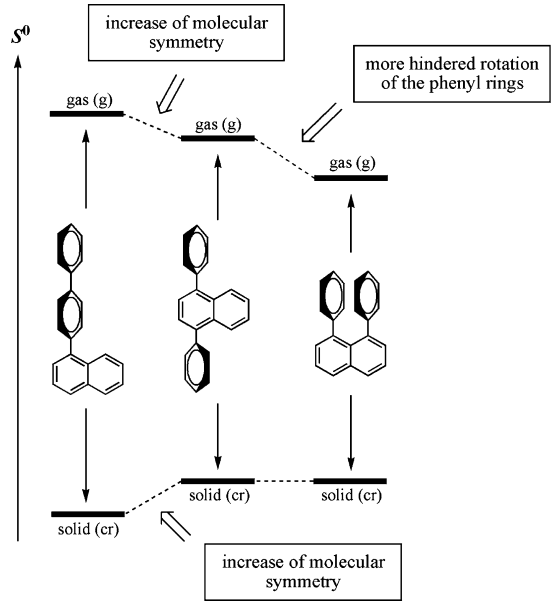

Figure 10. Entropic diagram showing the possible causes for the differentiation in $\Delta_{cr}^{g}S_m^0$ observed among the three isomers: 1-bPhN, 1,4-diPhN, and 1,8-diPhN.

Nevertheless, the 2-bPhN isomer does not seem to fit this rationalization in $\Delta_{cr}^{g}S_m^0$. The molecule has no symmetry (σ_{sym} = 1), and at a first glance, the phenyl rotors in the gas phase are not more hindered than the ones in the 1-bPhN isomer. Notwithstanding, the lower than expected $\Delta_{cr}^{g}S_m^0$ of 2-bPhN can also be related with hindered rotation of the phenyl substituents. Because of the β-phenyl relation, this isomer is more likely to present an enhanced electron delocalization (as it will be shown in a following section); a fact that is associated with higher ring coplanarity and should increase the energetic penalty associated with internal phenyl rotation, thus lowering S^0(g). This in turn suggests a more planar molecular geometry for 2-bPhN, which can lead to some positional degeneracy in the crystal lattice, thus increasing S^0(cr).

dx.doi.org/10.1021/jp2111378 | J. Phys. Chem. B 2012, 116, 3557−3570

Relative to the 1,8-dibPhN and 1,2,3,4-TPhN isomers, the large difference in $\Delta_{cr}^{g}S_{m}^{0}$ can be mainly attributed to the different degree of hindered rotation of the phenyl substituents in the gaseous phase. The X-ray structures of both compounds are consistent with $\sigma_{sym} = 2$, and thus there should be no significant differentiation in $\Delta_{cr}^{g}S_{m}^{0}$ due to molecular symmetry. In the 1,2,3,4-TPhN isomer the two β-phenyl substituents are surrounded by two adjacent phenyl neighbors, being therefore highly hindered relative to internal rotation, whereas the torsional profiles of the two outer phenyl substituents in 1,8-dibPhN should have a considerably lower rotational barrier and resemble the one for biphenyl. As demonstrated by the X-ray structure of 1,8-dibPhN, the outer phenyls are significantly further away from each other than the phenyl substituents directly bonded to naphthalene. In this way, differentiation in $S^{0}(g)$ should mainly arise due to the significantly different internal rotations associated with the two highly hindered β-phenyl substituents in 1,2,3,4-TPhN, and the two less hindered outer phenyl rings in 1,8-dibPhN.

The $\Delta_{cr}^{g}S_{m}^{0}$ data obtained in this work was fitted to a semiempirical additive model analogous to the one proposed recently for estimation of $\Delta_{cr}^{g}S_{m}^{0}$ in polyphenylbenzenes.[60] It was found that the previous model describes quite well the presented set of data for $\Delta_{cr}^{g}S_{m}^{0}$ (including naphthalene and seven phenylnaphthalenes studied), by the following equation:

$$\Delta_{cr}^{g}S_{m}^{0} = a + bn(\mathrm{Ph}) - cR\ln(\sigma_{sym}) + dn(\alpha/\beta\text{-phenyl/biphenyl}) + en(\text{peri-}\alpha\text{-phenyl}) \quad (9)$$

where a, b, c, d, and e are fitting parameters; σ_{sym} is the external symmetry number of the molecule, which corresponds to the number of unique orientations of the rigid molecule that only interchange identical atoms; n(Ph) is the total number of phenyl substituents; $n(\alpha/\beta$-phenyl/biphenyl) is the number of α and β phenyl substituents with zero phenyl neighbors (e.g., the two phenyls in 1,4-diPhN or the phenyl in 2-PhN), plus those that are bonded to another phenyl ring (e.g., the outer phenyl of 1-bPhN or 2-bPhN); n(*peri*-α-phenyl) is the number of α phenyl substituents with one adjacent *peri* phenyl neighbor (e.g., the two phenyls in 1,8-diPhN). Symmetry numbers, σ_{sym}, were taken from the X-ray crystallographic structures and/or from the MP2/cc-pVDZ optimized geometries as: naphthalene (4),[39] 2-PhN (1), 1-bPhN (1), 2-bPhN (1), 1,4-diPhN (2), 1,8-diPhN (2), 1,8-dibPhN (2), 1,2,3,4-TPhN (2).[29] The parameters d and e take into account the respective contributions from hindered rotation relative to the most hindered rotor, the β-phenyl in 1,2,3,4-TPhN. Applying a least-squares method, the values for the fitting parameters were found to be: $a = 187.1$ J·K^{-1}·mol^{-1}, $b = 9.7$ J·K^{-1}·mol^{-1}, $c = 1.5$, $d = 18.3$ J·K^{-1}·mol^{-1}, and $e = 14.9$ J·K^{-1}·mol^{-1}, giving an average error between the experimental and estimated $\Delta_{cr}^{g}S_{m}^{0}$ values of 2.4 J·K^{-1}·mol^{-1} (approximately 1% deviation). The compound 2-bPhN is clearly an outsider, and therefore was not considered in the fitting. For 2-bPhN to be part of the correlation, a contribution of ca. -13 J·K^{-1}·mol^{-1} for its $\Delta_{cr}^{g}S_{m}^{0}$ should be considered. Curiously, this value is very near $-R\ln(4)$, the contribution that is to be expected if 2-bPhN presents a structural degeneracy in the crystal lattice consistent with a planar linear molecule, for which $\sigma_{sym} = 4$. Unfortunately, suitable crystals of 2-bPhN for X-ray diffraction could not be obtained, in order to confirm this hypothesis. Interestingly, the value of c (constant multiplying the factor $R\cdot\ln(\sigma_{sym})$) is very similar to the one observed in our previous work concerning polyphenylbenzenes ($c = 1.4$).[60] As referred to that paper, this result suggests that symmetry leads to entropic differentiation both in crystal and gas phases and that its influence should be more correctly described in terms of continuous symmetry numbers.[50,59,60]

By nature, the intermolecular interactions in these compounds are mostly of the van der Waals type. Hence, the cohesive energy of the solid is expected to depend substantially on the available free molecular surface for interaction, with a higher intermolecular surface increasing the likelihood of short atomic contacts, thus contributing to stronger intermolecular interactions. In fact, for the $C_{22}H_{16}$ isomers the enthalpy of sublimation increases in the order: 1,8-diPhN < 1,4-diPhN < 1-bPhN ≈ 2-bPhN, which nicely follows the increase in molecular surface area. 1,8-diPhN has two blocked aromatic π faces, which leads to a decrease of the cohesive energy. The biphen-4-yl isomers are the ones with larger surface areas, in agreement with their greater $\Delta_{cr}^{g}H_{m}^{0}$ in this series. The 1,4-diPhN isomer is an intermediate case, since both phenyl substituents are bonded to the α position of naphthalene, which reduces slightly the volume extension of the aromatic π clouds relative to 1-bPhN and 2-bPhN. A similar trend is observed for the $C_{34}H_{24}$ isomers (1,8-dibPhN and 1,2,3,4-TPhN). In 1,2,3,4-TPhN only two π faces from a total out of eight are arising from the four phenyl groups, which hence are free to interact intermolecularly, whereas in 1,8-dibPhN, there are four unblocked π faces, and an increased extension of electron density due to the biphen-4-yl relation of the phenyl substituents. Moreover, as more phenyl substituents cluster around naphthalene, the less prone the naphthyl moiety is to participate in significant van der Waals intermolecular contacts. This explains the significantly higher $\Delta_{cr}^{g}H_{m}^{0}$ for the 1,8-dibPhN isomer. Linear correlations were obtained by plotting $\Delta_{cr}^{g}H_{m}^{0}$ as a function of the number of phenyl substituents in naphthalene for the following series: A, naphthalene, 2-PhN, and 2-bPhN ($R^2 = 0.9995$); B, naphthalene, 1,8-diPhN, and 1,8-dibPhN ($R^2 = 0.9999$). This indicates the existence of a simple additive pattern in intermolecular interactions in this class of compounds as the number of structurally similar phenyl rings is incremented.

Similar findings, respecting enthalpies of sublimation, were observed in our previous work concerning the related series of polyphenylbenzenes.[60]

Gas Phase Energetics. *Estimation of $\Delta_f H_m^0(g)$ for 1-Phenylnaphthalene.* The experimental determination of $\Delta_f H_m^0(g)$ of 1-phenylnaphthalene was not possible, since the purification of this compound to the required standards was not successfully achieved. Considering that in α-phenylnaphthalenes conjugation between the naphthyl and phenyl moieties is very weak (support for this fact comes from UV−vis and ^{1}H NMR spectroscopy[18,65,66]), estimation by an additive method was applied. The X-ray structures and optimized gas phase geometries at B3LYP/6-311++G(d,p) and MP2/cc-pVDZ levels of theory for the α-phenylnaphthalenes studied indicate a phenyl-naphthyl dihedral angle near 60°, far away from coplanarity, in all the cases. Therefore, the two homodesmotic gas phase reactions presented in Figure 11 should be nearly athermal, in accordance with what is expected if the energetic factors are additive. Our computational results support this observation, giving values of $\Delta_r E_{el}$(g, 0 K), in kJ·mol^{-1}, of 0.3 (HR1) and 0.0 (HR2) at the B3LYP/6-311++G(d,p), and of

dx.doi.org/10.1021/jp2111378 | J. Phys. Chem. B 2012, 116, 3557−3570

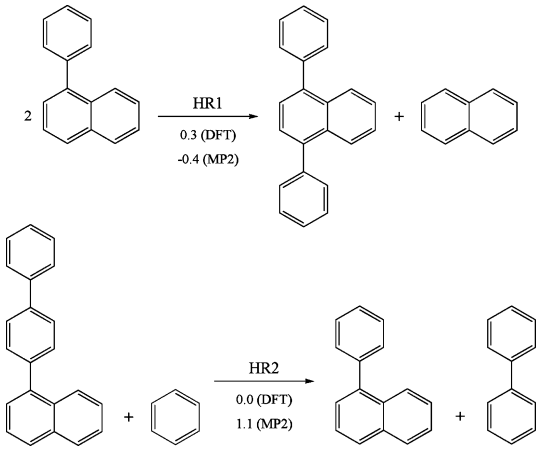

Figure 11. Homodesmotic gas phase reactions used for the estimation of $\Delta_f H^0_m(g)$ for 1-PhN. These reactions should be practically athermal, as supported by B3LYP/6-311++G(d,p) (DFT) and SCS-MP2/cc-pVDZ (MP2) calculations. Values of $\Delta_r E_{el}$(g, 0 K) in kJ·mol^{-1}.

−0.4 (HR1) and 1.1 (HR2) at the SCS-MP2/cc-pVDZ levels of theory.

Hence, $\Delta_f H^0_m$(1-PhN, g) = (252.3 ± 3.4) kJ·mol^{-1} was derived, as the resulting mean value from HR1 (252.9 ± 2.3) and HR2 (251.8 ± 4.4), assuming $\Delta_{HR} H^o_m$ (g) = 0.0 kJ·mol^{-1} for both reactions. The experimental values, in kJ·mol^{-1}, of $\Delta_f H^0_m$(benzene, g) = (82.9 ± 0.9),[47] and $\Delta_f H^0_m$(biphenyl, g) = (182.0 ± 0.7)[67] were used.

General Overview. The values of $\Delta_f H^0_m$(cr) for all the compounds presented in Table 6, except for 1-PhN, were determined by combustion calorimetry. In this way, for the calculation of the uncertainties in $\Delta_r H^0_m(g)$ for all the forthcoming reactions, the uncertainties related to the calibration of the calorimeters and the formation of CO_2(g) and H_2O(l) in the course of the corresponding combustion reactions can be ignored since these contributions cancel out in the homodesmotic reactions used.

Before proceeding with the analysis of gas phase energetics it is worth noting the significant similarity that was observed between the X-ray and optimized MP2/cc-pVDZ molecular structures, for the cases where both of them could be obtained. Moreover, due to the relatively low molecular flexibility of these systems, one should not expect to observe noteworthy deviations between the equilibrium structures adopted in the crystal and gas phases. These observations suggest that the X-ray structures can be used in order to give some support to gas phase energetics in the discussion that follows.

Figure 12 presents a general homodesmotic separation reaction scheme that can be used to compare gas phase energetics among the phenylnaphthalenes studied, and Table 7 summarizes the experimental results for $\Delta_{sep} H^0_m$ at T = 298.15 K.

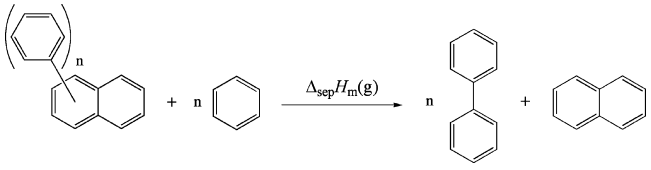

Figure 12. General gas phase separation reaction for the phenylnaphthalenes studied.

Table 7. Experimental Results for $\Delta_{sep} H^0_m$, at T = 298.15 K, for the Homodesmotic Reaction Scheme Presented in Figure 12

compound	n	$\Delta_{sep} H^0_m$(g)/kJ mol^{-1}
1-PhN	1	−2.6 ± 3.9
2-PhN	1	1.7 ± 2.0
1-bPhN	2	−2.1 ± 2.5
2-bPhN	2	10.3 ± 2.5
1,4-diPhN	2	−6.4 ± 2.8
1,8-diPhN	2	−21.1 ± 2.7
1,8-dibPhN	4	−8.2 ± 3.2
1,2,3,4-TPhN	4	−16.9 ± 2.9

Using this approach, some direct comparisons can be made between all the compounds studied, with positive/negative $\Delta_{sep} H^0_m$ values indicating that the total interaction between all phenyl groups in naphthalene is stabilizing/destabilizing relative to separated biphenyl and naphthalene.

These results clearly indicate significant energetic differentiation among the compounds studied.

Conjugation in β-Phenylnaphthalenes Leads to Significant Energetic Stabilization. As referred before, the results obtained in this and other works point to a lack of conjugation between naphthalene and phenyl substituents in the α position. The main cause for this phenomenon may be related with the significant steric interaction between the *ortho* hydrogen of the phenyl rings and the adjacent *peri* hydrogen of naphthalene, which prevents the achievement of more planar geometries (smaller angle Φ(Ph−naphthyl)), and thus a significant overlap of electron density that would lead to enhanced electron delocalization. Table 8 presents the values for the ring−ring dihedral angles, Φ(ring−ring), obtained in this work by X-ray crystallography and theoretical calculations at the MP2/cc-pVDZ level of theory, with respect to all the ring−ring bonds in the compounds studied. The Ph−naphthyl dihedral angles for the α-phenylnaphthalenes are of about 60°, while β-phenylnaphthalenes and biphenyl derivatives present substantially lower ring−ring dihedral angles, for instance Φ(Ph-Ph) = (44.4 ± 1.2)° in gaseous biphenyl.[68]

Table 8. Ring−Ring Dihedral Angles, Φ(ring−ring), for All the Ring−Ring Bonds for the Compounds Considered in This Work, Derived from X-ray Crystallography and Theoretical Calculations at the MP2/cc-pVDZ Level of Theory

	Φ(ring−ring)/deg	
compound	X-ray	MP2
1-PhN	–	58
2-PhN	–	42
1-bPhN[a]	57; 28	57; 42
2-bPhN	–	42; 42
1,4-diPhN	53; 52	58; 58
1,8-diPhN	66; 67	56; 56
1,8-dibPhN[a]	74; 61/30; 42	–
1,2,3,4-TPhN[b]	74; 71/64; 66	–

[a]Left values: Ph−naphthyl torsions/right values: Ph−Ph torsions. [b]Left values: α-phenyl substituents/right values: β-phenyl substituents.

From Table 6 one can see that in the gas phase 1-bPhN is slightly more stable than 1,4-diPhN. The difference in $\Delta_f H^0_m(g)$ for these two isomers can be related to the different molecular

dx.doi.org/10.1021/jp2111378 | J. Phys. Chem. B 2012, 116, 3557−3570

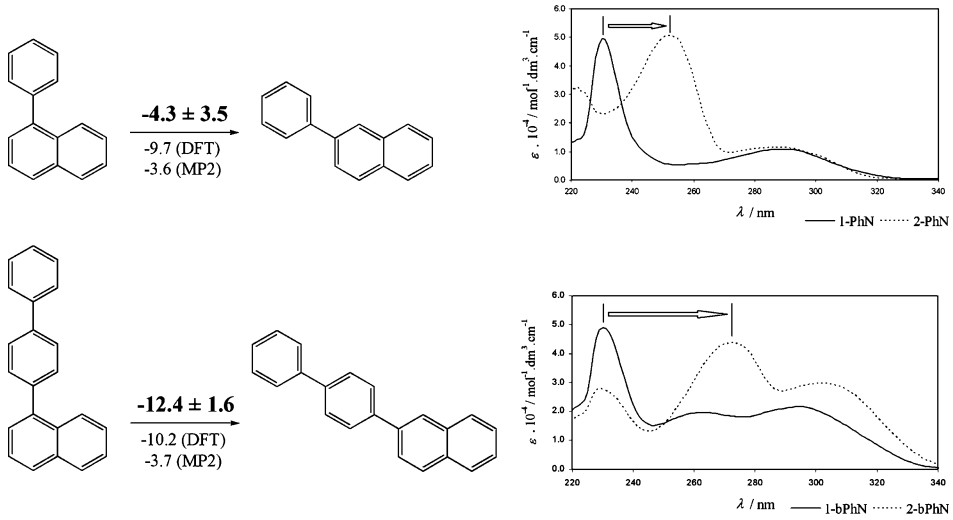

Figure 13. Gas phase isomerization reactions for α- and β-phenylnaphthalenes, and respective UV−vis spectra, recorded in CH_2Cl_2, at T = 298.1 K. Enthalpic stabilization is associated with a bathochromic shift. Experimental (in bold), B3LYP/6-311++G(d,p) (DFT), and SCS-MP2/cc-pVDZ (MP2) values in kJ·mol^{-1} are presented.

environment of the phenyl substituents. While in 1-bPhN one phenyl ring has a biphenyl-like relation, for which Φ(Ph-Ph) = 28° (X-ray), in 1,4-diPhN both phenyl substituents are bonded to the α position of naphthalene, with Φ(Ph-naphthyl) = 52° (X-ray). This is a good indication that a main factor that energetically distinguishes these two isomers in the gas phase is the degree of planarity of the phenyl rings.

The β-phenylnaphthalenes studied, 2-PhN and 2-bPhN, are significantly more stable than their corresponding α isomers, with the stabilization being more pronounced in 2-bPhN. Figure 13 presents the experimental gas phase isomerization enthalpies, $\Delta_{isom}H^0_m(g)$, at T = 298.15 K, and the theoretically calculated electronic isomerization energies, $\Delta_{isom}E_{el}(g)$, at T = 0 K (ZPE and thermal correction contributions were neglected since they are usually of little importance in an isomerization reaction), alongside with their respective UV−vis spectra.

Figure 13 shows that a significant bathochromic shift in the UV−vis spectra is observed on going from the α to the β isomers. It can also be observed that on going from 2-PhN to 2-bPhN the λ_{max} varies significantly, whereas from 1-PhN to 1-bPhN it is virtually unchanged. As can be seen in Table 8, β-phenylnaphthalenes tend to present lower values of Φ(Ph-naphthyl), which is consistent with greater conjugation and stability. The bathochromic shift is more pronounced for 2-bPhN, being nicely accompanied by a more negative $\Delta_{isom}H^0_m(g)$. These results constitute a good indication that enthalpic stability in phenylnaphthalenes is related to the extent of conjugation between the phenyl and naphthyl moieties in these molecules. Nevertheless, the theoretical results are not able to distinguish between the two isomerization reactions. The fact that both the enthalpic stabilization and bathochromic shift are considerably more pronounced in 2-bPhN suggests that a significant electron delocalization, not totally accounted for by the theoretical results, exists in this molecule and extends through the whole π system. In reality, the orbital overlap between the various rings in 2-bPhN appears to be more extensive than considered by the computational calculations. In this way, a geometry more closer to planarity than the one obtained computationally may be expected for this molecule.

Intramolecular T-Shaped Aromatic Interaction in 1,8-Di([1,1′-biphenyl]-4-yl)naphthalene. Figure 14 presents two

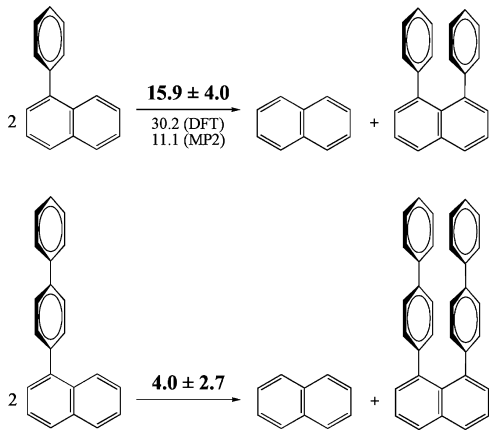

Figure 14. Homodesmotic gas phase reactions used for the evaluation of the intramolecular aromatic interactions in 1,8-diPhN and 1,8-dibPhN. Experimental (in bold), B3LYP/6-311++G(d,p) (DFT), and SCS-MP2/cc-pVDZ (MP2) values in kJ·mol^{-1} are reported.

homodesmotic reactions planned with the intention of evaluating experimentally and computationally the intramolecular interaction between the adjacent phenyl substituents in 1,8-diPhN and 1,8-dibPhN. The experimental results for the standard gas phase enthalpies of reaction, $\Delta_rH^0_m(g)$, at T = 298.15 K, and electronic energies of reaction, $\Delta_rE_{el}(g)$, at T = 0 K, are presented (ZPE and thermal corrections were neglected since they are usually of little importance in a homodesmotic reaction).

A repulsive interaction is clearly observed between the two phenyl substituents in 1,8-diPhN. Because of their close proximity favorable intramolecular aromatic interactions could be established. However, the two aromatic rings are too close, and the repulsive short-range contribution dominates the interaction at this distance. In the crystal structure of 1,8-diPhN[28] one can observe that the distance between the centroids of the two Ph rings is of 3.51 Å, which matches the theoretical calculated equilibrium distance of the parallel displaced benzene dimer,[8−12] but the distance between the two carbon atoms directly bonded to naphthalene is only 2.98 Å. The enthalpic destabilization then probably arises from this

dx.doi.org/10.1021/jp2111378 | J. Phys. Chem. B 2012, 116, 3557−3570

close proximity at the base of the rings, and from the slight geometric deformation of the molecule, which is more perceived in the increase of the angle between the phenyl rings and naphthalene and in the increase of the Ph−naphthyl dihedral angles (see Table 8).

Figure 15 illustrates the parallel displaced orientation that the two phenyl rings adopt relative to each other in the crystal

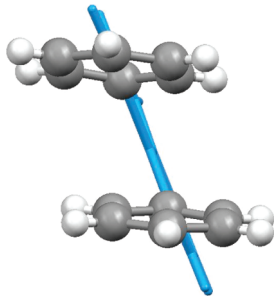

Figure 15. Schematic picture showing the parallel displaced orientation of the phenyl substituents in the crystal phase of 1,8-diPhN.[28]

phase of 1,8-diPhN.[28] Nevertheless, the fact that the DFT result is significantly more positive than the experimental and MP2 data indicates that attractive dispersive contributions are significant for the total interaction energy, which is typical of a parallel displaced aromatic interaction.[8−12] It is well recognized that most DFT methods, including B3LYP, are not able to properly describe the attractive components of van der Waals interactions.[8]

Since 1,4-diPhN can practically be viewed as a combination of two noninteracting aromatic rings, the 1,4-diPhN → 1,8-diPhN isomerization reaction is also a good way of evaluating the intramolecular interaction in 1,8-diPhN. The values of $\Delta_r H^0_m(g)$ for this reaction, in kJ·mol^{-1}, are 14.7 ± 2.3 (experimental), 29.9 (B3LYP), and 11.5 (SCS-MP2). As expected, these results are very similar to the ones obtained for the first homodesmotic reaction presented in Figure 14.

There is no reason for the interaction between the two phenyl substituents directly bonded to naphthalene in 1,8-dibPhN to be less repulsive than in 1,8-diPhN. Their respective crystallographic structures show that the geometric parameters relative to this pair of rings (centroid−centroid distance, bond lengths and angles, angles and dihedral angles relative to naphthalene) are very similar for both molecules. Hence, the significantly lower $\Delta_r H^0_m(g)$ observed for the second homodesmotic reaction presented in Figure 14 is probably due to an attractive aromatic intramolecular interaction between the two outer phenyl rings in 1,8-dibPhN. The X-ray crystal structure of 1,8-dibPhN is consistent with this finding and suggests an interaction geometry that approaches the T-shaped structure of the benzene dimer. As shown in Figure 16, the two outer phenyl rings in this molecule can establish two C−H···π intramolecular contacts. This explains why the two Ph−Ph dihedral angles, as shown in Table 8, are significantly different in this molecule. One ring tends to become perpendicular relative to the other, increasing Φ(Ph−Ph), in order to maximize the two C−H···π contacts. The intramolecular distances are shown in Figure 16 and are within the typical values for this type of interaction.[8−12,69]

The aromatic interaction enthalpy can then be easily calculated as the difference in $\Delta_r H^0_m(g)$ for the two reactions

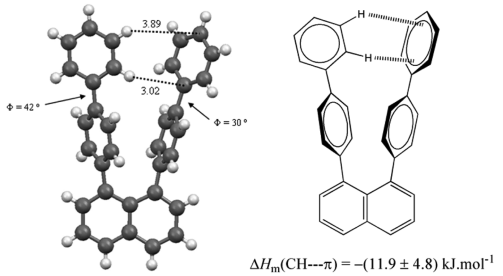

Figure 16. Intramolecular T-shaped (CH···π) aromatic interaction between the outer phenyl rings in 1,8-dibPhN: X-ray crystallographic structure (left) and schematic representation (right). The two C−H···π interaction distances (in Å) and the two Ph−Ph dihedral angles are shown.

presented in Figure 14, which gives ΔH_m(CH···π) = −(11.9 ± 4.8) kJ·mol^{-1}, in gaseous 1,8-dibPhN. This value is in perfect agreement with recent high-level *ab initio* calculations at the CCSD(T) level of theory at the basis set limit, for T-shaped benzene dimers.[8−12] The true equilibrium geometry for this intramolecular interaction in the crystal phase of 1,8-dibPhN is presented in Figure 17. Strictly speaking, this is not a typical T-

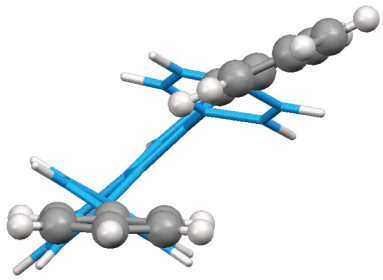

Figure 17. Schematic picture showing the relative orientation of the two outer phenyl rings in the crystal phase of 1,8-dibPhN.

shaped structure, but the two interacting C−H bonds of one ring still adopt a favorable orientation toward the π cloud of the other aromatic ring. The molecular geometry in the gas phase should closely resemble the one adopted in the crystal; however, the absence of an intermolecular potential may allow the establishment of a more perpendicular T-shaped structure for this interaction in the gas phase. Owing to the nature of the molecules shown in Figure 14, the existence of the aromatic interaction between the outer phenyls in 1,8-dibPhN is the most obvious explanation to the difference observed in $\Delta_r H^0_m(g)$. The outer rings in this molecule are relatively far away from each other, and thus it seems logical that they adopt a structure that more resembles the T-shaped one in order to maximize the intramolecular interaction. A geometry more closer to parallel displaced would increase the distance of short contacts between the rings (the X-ray structure indicates a centroid-centroid distance of 5.2 Å) and probably dilute the interaction to a marginal value, reducing the difference in $\Delta_r H^0_m(g)$ for the two reactions. According to recent theoretical studies, the calculated Potential Energy Surface (PES) for the parallel displaced benzene dimer points to an interaction energy, ΔE_{int}, at these distances of ≈2−3 kJ·mol^{-1},[8,10] well below 11.9 kJ·mol^{-1} as indicated by our experimental results.

1,2,3,4-Tetraphenylnaphthalene. The experimental results indicate that the four adjacent phenyl substituents in the molecule of 1,2,3,4-TPhN do not lead to significant repulsive

dx.doi.org/10.1021/jp2111378 | J. Phys. Chem. B 2012, 116, 3557−3570

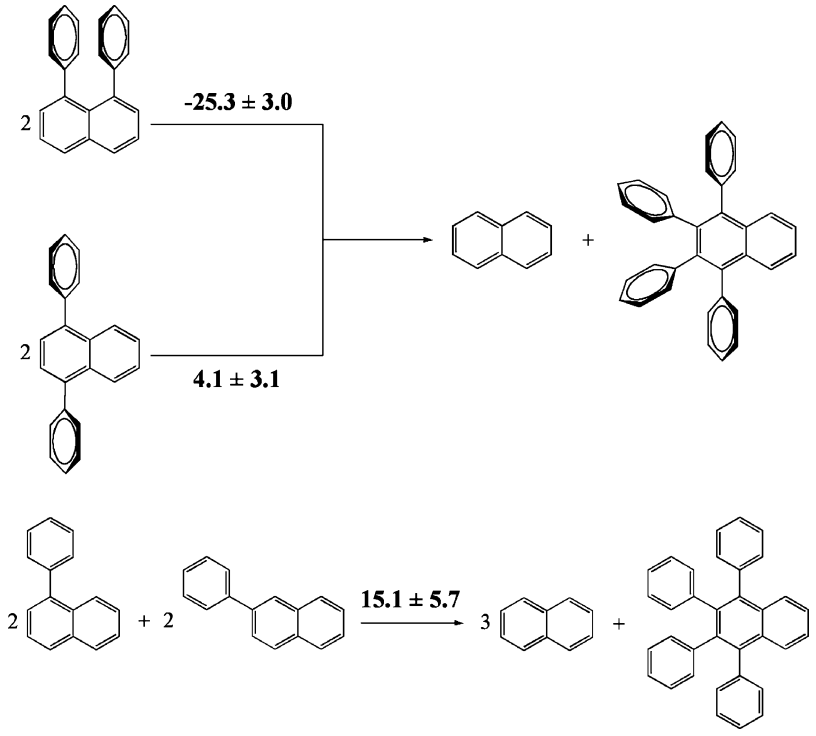

Figure 18. Homodesmotic gas phase reaction schemes used for the evaluation of energetics in 1,2,3,4-TPhN. Experimental values in kJ·mol^{-1}.

steric interactions. The first homodesmotic reaction scheme in Figure 18 indicates that intramolecular repulsions are much more prevalent when the phenyl groups have a *peri* relation, like in 1,8-diPhN. In this situation, the phenyl rings are very close to each other and overlap considerably more electron density than the phenyl substituents in 1,2,3,4-TPhN. This scheme also indicates that, within experimental error, the energetics of 1,2,3,4-TPhN can be approximated by the additive contribution of one naphthalene and four α-phenyl substituents. This can also be observed by plotting $\Delta_f H^0_m(g)$ as a function of the number of Ph substituents for the following series: naphthalene, 1-PhN, 1,4-diPhN, and 1,2,3,4-TPhN. This yields a straight line with R^2 = 0.99996, thus supporting the validity of the group additivity assumption in these compounds.

When the two α-phenyl and two β-phenyl relations in 1,2,3,4-TPhN are considered in a homodesmotic scheme (last reaction in Figure 18), an enthalpic destabilization is observed. In 1,2,3,4-TPhN, each β-phenyl substituent is surrounded by two phenyl neighbors, and thus they are forced to adopt a more perpendicular geometry relative to the naphthalene plane, a fact that is proved by their high Ph-naphthyl dihedral angles (see Table 8). This departure from planarity shall disrupts the conjugation between the β-phenyl and naphthyl moieties that was observed in 2-PhN, and is probably the main source of destabilization in 1,2,3,4-TPhN. Hence, with respect to energetics, the β-phenyls in this molecule can be regarded as α-phenyls. The combination of these findings precludes the existence of strong repulsive interactions in the molecule of 1,2,3,4-TPhN. Moreover, a significant deformation of the naphthalene ring is not observed in the crystal structure of this compound.[29] Nevertheless, because $\Delta_r H^0_m(g)$ is slightly positive for the homodesmotic reaction presented in Figure 18 that includes 1,4-diPhN one cannot discard the existence of a small repulsive contribution in 1,2,3,4-TPhN. In principle, the phenyl rings in 1,2,3,4-TPhN can be compared with *o*-phenyl substituents in benzene. As noted in a previous work, the presence of *o*-phenyl rings in benzene do not impose significant destabilization in polyphenylbenzenes.[60] Despite being relatively close to each other (prone to steric hindrance), the contribution of dispersive interactions between the rings, typical of aromatic $\pi\cdots\pi$ interactions, prevents a noteworthy destabilization of these molecules. This partial cancellation of effects thus allows the rings in 1,2,3,4-TPhN to be treated like virtually noninteracting α-phenyls.

CONCLUSION

The relationships between structure and energetics in a series of relatively simple phenylnaphthalenes has been explored, experimentally and theoretically, in order to properly characterize and quantify the relevant fundamental chemical aspects that lead to enthalpic and entropic differentiation among these compounds. It was found that the differences in the entropy of sublimation can be rationalized in terms of molecular symmetry and hindered internal rotation of the phenyl substituents. Higher molecular symmetry increases $S^0(cr)$ and/or decreases $S^0(g)$, thus decreasing $\Delta^g_{cr}S^0_m$, while more hindered rotations decrease $S^0(g)$, and consequently $\Delta^g_{cr}S^0_m$. The trend in the enthalpies of sublimation can be understood by considering the surface area of the molecules, showing that as the surface area, and hence the likelihood to establish short atomic contacts, increases the cohesive energy of the crystalline solid becomes stronger.

With respect to molecular energetics, it was found that conjugation in α-phenylnaphthalenes is practically absent, leading to a scenario of group transferability in $\Delta_f H^0_m(g)$ for these compounds. On the other hand, a significant enthalpic stabilization, due to enhanced electron delocalization, was observed in β-phenylnaphthalenes, a phenomenon that is particularly pronounced in 2-bPhN. The global results suggest that enthalpic stability in these systems is strongly related with

dx.doi.org/10.1021/jp2111378 | J. Phys. Chem. B 2012, 116, 3557−3570

the dihedral angles adopted by the various phenyl substituents, with lower dihedrals being associated with increased molecular stability. While the intramolecular interaction between the two phenyl substituents in 1,8-diPhN is strongly repulsive, a stabilizing aromatic interaction between the two outer phenyl rings in 1,8-dibPhN was found, and quantified on pure experimental grounds as $-(11.9 \pm 4.8)$ kJ·mol^{-1}. The X-ray crystallographic structure of 1,8-dibPhN corroborates this finding and indicates that the rings adopt a quasi T-shaped structure, establishing two C−H···π intramolecular contacts. Intramolecular repulsion was found to be of little importance in 1,2,3,4-TPhN. However, the existence of adjacent phenyl substituents precludes the achievement of more planar geometries of the β-phenyl rings, canceling the enthalpic stabilization associated with the phenyl−naphthyl conjugation at this position.

This rationale derived from the study of relatively simple compounds can be of great assistance for a complete and robust characterization of some fundamental aspects of chemistry that influence the behavior of more complex chemical systems.

■ ASSOCIATED CONTENT

Supporting Information

Detailed description of the techniques, detailed X-ray crystallography, combustion, and sublimation results, UV−vis spectra for 1-PhN, 2-PhN, 1-bPhN, and 2-bPhN in CH_2Cl_2, at T = 298.1 K, and total electronic energies obtained from the optimized structures for benzene, biphenyl, naphthalene, 1-PhN, 2-PhN, 1-bPhN, 2-bPhN, 1,4-diPhN, and 1,8-diPhN. This material is available free of charge via the Internet at http://pubs.acs.org.

■ AUTHOR INFORMATION

Corresponding Author

*E-mail: lbsantos@fc.up.pt. Telephone: +351 220402536. Fax: +351 220402520.

Notes

The authors declare no competing financial interest.

■ ACKNOWLEDGMENTS

Thanks are due to Fundação para a Ciência e Tecnologia (FCT) and Programa Operacional Ciência e Inovação 2010 (POCI 2010) supported by the European Community Fund FEDER for the financial support to Project POCI/QUI/61873/2004. C.F.R.A.C.L., M.A.A.R., and B.S. also thank FCT and the European Social Fund (ESF) under the third Community Support Framework (CSF) for the award of the research grants: SFRH/BD/29394/2006, SFRH/BD/60513/2009, and SFRH/BPD/38637/2007, respectively.

■ REFERENCES

(1) Berresheim, A. J.; Müller, M.; Müllen, K. *Chem. Rev.* **1999**, *99*, 1747−1786.
(2) Kertesz, M.; Choi, C. H.; Yang, S. *Chem. Rev.* **2005**, *105*, 3448−3481.
(3) Minato, H.; Higosaki, N.; Isobe, C. *Bull. Chem. Soc. Jpn.* **1969**, *42*, 779−781.
(4) Song, S.; Lee, H.; Jin, Y.; Ha, Y. M.; Bae, S.; Chung, H. Y.; Suh, H. *Bioorg. Med. Chem. Lett.* **2007**, *17*, 461−464.
(5) Kawazoe, K.; Yutoni, A.; Tamemoto, K.; Yuasa, S.; Shibata, H.; Higuti, T.; Takaishi, Y. *J. Nat. Prod.* **2001**, *64*, 588−591.
(6) Cozzi, F.; Siegel, J. S. *Pure Appl. Chem.* **1995**, *67*, 683−689.
(7) Hunter, C. A.; Sanders, J. K. M. *J. Am. Chem. Soc.* **1990**, *112*, 5525−5534.
(8) Tsuzuki, S. *Struct. Bonding (Berlin)* **2005**, *115*, 149−193.
(9) Hunter, C. A.; Lawson, K. R.; Perkins, J.; Urch, C. J. *J. Chem. Soc. Perkin Trans. 2* **2001**, 651−669.
(10) Sinnokrot, M. O.; Sherrill, C. D. *J. Phys. Chem. A* **2004**, *108*, 10200−10207.
(11) Sinnokrot, M. O.; Sherrill, C. D. *J. Am. Chem. Soc.* **2004**, *126*, 7690−7697.
(12) Tsuzuki, S.; Honda, K.; Uchimaru, T.; Mikami, M.; Tanabe, K. *J. Am. Chem. Soc.* **2000**, *122*, 3746−3753.
(13) Guckian, K. M.; Schweitzer, B. A.; Ren, R. X.−F.; Sheils, C. J.; Tahmassebi, D. C.; Kool, E. T. *J. Am. Chem. Soc.* **2000**, *122*, 2213−2222.
(14) Burley, S. K.; Petsko, G. A. *Science* **1985**, 23−28.
(15) Sygula, A.; Fronczek, F. R.; Sygula, R.; Rabideau, P. W.; Olmstead, M. M. *J. Am. Chem. Soc.* **2007**, *129*, 3842−3843.
(16) Anelli, P. L.; Spencer, N.; Stoddart, J. F. *J. Am. Chem. Soc.* **1991**, *113*, 5131−5133.
(17) Rocha, M. A. A.; Lima, C .F. R. A. C.; Santos, L. M. N. B. F. *J. Chem. Thermodyn.* **2008**, *40*, 1458−1463.
(18) Lima, C. F. R. A. C.; Rodriguez-Borges, J. E.; Santos, L. M. N. B. F. *Tetrahedron* **2011**, *67*, 689−697.
(19) Bruker; Smart APEX (version 5.62), SAINT (Version 6.02), SHELXTL (Version 6.10), and SADABS (Version 2.03). Bruker AXS Inc.: Madison, WI, 2004.
(20) McArdle, P.; Gilligan, K.; Cunningham, D.; Dark, R.; Mahon, M. *CrystEngComm* **2004**, *6*, 303−309.
(21) Sheldrick, G. M. SHELXS97 and SHELXL97. Program for Crystal Structure Refinement; University of Göttingen: Göttingen, Germany, 1997.
(22) Johnson, C. K.; Burnett, M. N. ORTEPIII for Windows; University of Glasgow: Glasgow, U.K., 1998.
(23) Spek, A. L. *J. Appl. Crystallogr.* **2003**, *36*, 7−13.
(24) Gundry, H. A.; Harrop, D.; Head, A. J.; Lewis, G. B. *J. Chem. Thermodyn.* **1969**, *1*, 321−332.
(25) Bickerton, J.; Pilcher, G.; Al-Takhin, G. *J. Chem. Thermodyn.* **1984**, *16*, 373−378.
(26) Ribeiro da Silva, M. A. V.; Pilcher, G.; Santos, L. M. N. B. F.; Lima, L. M. S. S. *J. Chem. Thermodyn.* **2007**, *39*, 689−697.
(27) Santos, L. M. N. B. F.; Silva, M. T.; Schröder, B.; Gomes, L. *J. Therm. Anal. Calorim.* **2007**, *89*, 175−180.
(28) Tsuji, R.; Komatsu, K.; Takeuchi, K.; Shiro, M.; Cohen, S.; Rabinovitz, M. *J. Phys. Org. Chem.* **1993**, *6*, 435−444.
(29) Ojala, W. H.; Gustafson, H. L.; Ojala, C. R. *Acta Crystallogr.* **1994**, *C50*, 1602−1604.
(30) Johnson, W. H. *J. Res. Natl. Bur. Stand.* **1975**, *79A*, 425−429.
(31) Washburn, E. W. *J. Res. Natl. Bur. Stand.* **1933**, *10*, 525−558.
(32) Hubbard, W. N.; Scott, D. W.; Waddington, G. In *Experimental Thermochemistry*; Rossini, F. D., Ed.; Interscience: New York, 1956; Vol. *1*, Chapter 5.
(33) Good, W. D.; Scott, D. W. In *Experimental Thermochemistry*; Skinner, H. A., Ed.; Interscience: New York, 1962; Vol. *2*, Chapter 2.
(34) Wieser, M. E. *Pure Appl. Chem.* **2006**, *78*, 2051−2066.
(35) Santos, L. M. N. B. F.; Lima, L. M. S. S.; Lima, C. F. R. A. C.; Magalhães, F. D.; Torres, M. C.; Schröder, B.; Ribeiro da Silva, M. A. V. *J. Chem. Thermodyn.* **2011**, *43*, 834−843.
(36) Frisch, M. J.; et al. *Gaussian 03*, revision C.02; Gaussian, Inc.: Pittsburgh, PA, 2004.
(37) Grimme, S. J. *J. Chem. Phys.* **2003**, *118*, 9095−9102.
(38) Allen, F. H.; Kennard, O.; Watson, D. G.; Orpen, G.; Brammer, L.; Taylor, R. *J. Chem. Soc. Perkin Trans. 2* **1987**, S1.
(39) Oddershede, J.; Larsen, S. *J. Phys. Chem. A* **2004**, *108*, 1057−1063.
(40) *CODATA Key Values for Thermodynamics*; Cox, J. D., Wagman, D. D., Medvedev, V. A., Eds.; Hemisphere: New York, 1989.
(41) Konicek, J.; Suurkuusk, J.; Wadsö, I. *Chem. Scr.* **1971**, *1*, 217−220.
(42) Suurkuusk, J.; Wadsö, I. *J. Chem. Thermodyn.* **1974**, *6*, 667−679.

(43) Santos, L. M. N. B. F.; Rocha, M. A. A.; Rodrigues, A. S. M. C.; Štejfa, V.; Fulem, M.; Bastos, M. *J. Chem. Themodyn.* **2011**, *43*, 1818−1823.
(44) Domalski, E. S.; Hearing, E. D. *J. Phys. Chem. Ref. Data* **1996**, *25*, 1−525.
(45) Merrick, J. P.; Moran, D.; Radom, L. *J. Phys. Chem. A* **2007**, *111*, 11683−11700.
(46) Monte, M. J. S.; Santos, L. M. N. B. F.; Fulem, M.; Fonseca, J. M. S.; Sousa, C. A. D. *J. Chem. Eng. Data* **2006**, *51*, 757−766.
(47) Roux, M. V.; Temprado, M.; Chickos, J. S.; Nagano, Y. *J. Phys. Chem. Ref. Data* **2008**, *37*, 1855−1996.
(48) Swendsen, R. H. *Entropy* **2008**, *10*, 15−18.
(49) Kramer, G. M.; Scouten, C. G.; Kastrup, R. V.; Ernst, E. R.; Pictroski, C. F. *J. Phys. Chem.* **1989**, *93*, 6257−6260.
(50) Estrada, E.; Avnir, D. *J. Am. Chem. Soc.* **2003**, *125*, 4368−4375.
(51) Brown, R. J. C.; Brown, R. F. C. *J. Chem. Educ.* **2000**, *77*, 724−731.
(52) Gilbert, A. S. *Thermochim. Acta* **2007**, *452*, 135−139.
(53) Abramowitz, R.; Yalkowsky, S. H. *Pharm. Res.* **1990**, *7*, 942−947.
(54) Lin, S.-K. *J. Chem. Inf. Comput. Sci.* **1996**, *36*, 367−376.
(55) Pinal, R. *Org. Biomol. Chem.* **2004**, *2*, 2692−2699.
(56) Watson, L. A.; Eisenstein, O. *J. Chem. Educ.* **2002**, *79*, 1269−1277.
(57) Wei, J. *Ind. Eng. Chem. Res.* **1999**, *38*, 5019−5027.
(58) Dannenfelser, R.-M.; Yalkowsky, S. H. *Ind. Eng. Chem. Res.* **1996**, *35*, 1483−1486.
(59) Breuer, J.; Avnir, D. *J. Chem. Phys.* **2005**, *122*, 074110−1−074110−10.
(60) Lima, C. F. R. A. C.; Rocha, M. A. A.; Melo, A.; Gomes, L. R.; Low, J. N.; Santos, L. M. N. B. F. *J. Phys. Chem. A* **2011**, DOI: 10.1021/jp207593s.
(61) Maczek, A. *Statistical Thermodynamics*; Oxford University Press: New York, 2008; p 19.
(62) Atkins, P.; de Paula, J. *Physical Chemistry*, 7th ed.; Oxford University Press: New York, 2002; p 650.
(63) Mayer, J. E.; Brunauer, S.; Mayer, M. G. *J. Am. Chem. Soc.* **1933**, *55*, 37−53.
(64) McQuarrie, D. A.; Simon, J. D. *Physical Chemistry: A Molecular Approach*; University Science Books: Sausalito, CA, 1997.
(65) House, H. O.; Koepsell, D. G.; Campbell, W. J. *J. Org. Chem.* **1972**, *37*, 1003−1011.
(66) House, H. O.; Magin, R. W.; Thompson, H. W. *J. Org. Chem.* **1963**, *28*, 2403−2406.
(67) Chirico, R. D.; Knipmeyer, S. E.; Nguyen, A.; Steele, W. V. *J. Chem. Thermodyn.* **1989**, *21*, 1307−1331.
(68) Almenningen, A.; Bastiansen, O.; Fernholt, L.; Cyvin, B. N.; Cyvin, S. J.; Samdal, S. *J. Mol. Struct.* **1985**, *128*, 59−76.
(69) Lima, C. F. R. A. C.; Sousa, C. A. D.; Rodriguez-Borges, J. E.; Melo, A.; Gomes, L. R.; Low, J. N.; Santos, L. M. N. B. F. *Phys. Chem. Chem. Phys.* **2010**, *12*, 11228−11237.